

Volume Changes of the Myosin Lattice Resulting from Repetitive Stimulation of Single Muscle Fibers

G. Rapp,* C. C. Ashley,# M. A. Bagni,§ P. J. Griffiths,# and G. Cecchi§

*University Laboratory of Physiology, Oxford OX1 3PT, England; §Dipartimento di Scienze Fisiologiche, Università degli Studi di Firenze, Florence I-50134, Italy; and #EMBL Outstation, Deutsches Elektronen-Synchrotron, D-22603 Hamburg, Germany

ABSTRACT Single muscle fibers at 1°C were subjected to brief tetani (20 Hz) at intervals of between 20 s and 300 s over a period of up to 2 h. A band lattice spacing increased during this period at a rate inversely dependent on the rest interval between tetani. Spacing increased rapidly during the first 10 tetani at a rate equivalent to the production of 0.04 mOsmol·liter⁻¹ of osmolyte per contraction, then continued to expand at a much slower rate. For short rest intervals, where lattice expansion was largest, spacing increased to a limiting value between 46 and 47 nm (sarcomere length 2.2 μ m), corresponding to accumulation of 30 mOsmol·liter⁻¹ of osmolytes, where it remained constant until repetitive stimulation was terminated. At this limiting spacing, force was reduced by up to 30%. The effect of lattice swelling on the lattice compression that accompanies isometric force recovery from unloaded shortening was to increase the compression, similar to that observed in hypotonic media at a similar spacing. During recovery from repetitive stimulation, spacing recompressed to its original value with a half-time of 15–30 min. These findings suggest that mechanical activity produces an increase in osmotic pressure within the cell as a result of product accumulation from cross-bridge and sarcoplasmic reticulum ATPases and glycolysis.

INTRODUCTION

The volume of a rested, relaxed skeletal muscle cell remains virtually constant, changes in sarcomere length being accompanied by very rapid compensatory adjustment of the cross-sectional area of the muscle fiber (Ashley et al., manuscript submitted for publication). However, both during and immediately after mechanical activity, many studies have reported a change in cell volume, but there is no clear agreement on whether this change represents an expansion or a compression. It has been shown, using an optical microscopy technique (Blinks, 1965), that the volume of skeletal muscle cells increases by up to 35% as a result of repeated tetanic contractions to the point of fatigue (Lännergren, 1990). On the other hand, individual contractions have been reported to cause a modest shrinkage of fiber volume (0.0075%; Abbott and Baskin, 1962; Baskin and Paolini, 1966) and a larger compression of myofilament lattice volume (3.5%; Cecchi et al., 1990) or a nonuniform swelling of up to 20% (Neering et al., 1991).

The equatorial x-ray diffraction pattern of skeletal muscle cells provides information about the radial distribution of mass in the A band of an intact muscle cell. As a result, dynamic changes in the radial spacing of the myofilaments may be calculated to a high degree of precision, and when combined with sarcomere length measurement, spacing changes arising from fiber shortening or lengthening can be compensated for, and thereby spacing changes arising from other causes can be studied in isolation. We have used this

method to examine what changes occur in A band lattice spacing during periods of repetitive stimulation. We find that the lattice undergoes an expansion at a rate determined by the rest interval between tetani. In addition, we have examined the effect of lattice swelling on the compressive radial forces acting during the recovery of isometric tension after a period of shortening at almost zero load (Cecchi et al., 1990; Bagni et al., 1994) and compared this with the behavior of fibers in which the lattice has been swollen to a similar extent by exposure to hypotonic media (Bagni et al., 1994).

MATERIALS AND METHODS

Preparation and protocol

Single intact muscle fibers were prepared from tibialis anterior muscles of *Rana temporaria*, using aluminium clips attached to the tendons to reduce series compliance. They were mounted between a fast force transducer and a moving coil stretcher motor, which were used to record force and control fiber length, respectively, during periods of isometric and isotonic contraction. Sarcomere length (determined by a laser diffractometer system; Cecchi et al., 1991) was adjusted to 2.25 μ m, close to the upper limit of the plateau region of the length-tension relationship, so that after a small amount of shortening associated with activation, any further period of active shortening permitted would occur at full overlap. Fibers were electrically excited to produce brief tetani by up to three brief current pulses at 50-ms intervals between platinum electrodes mounted in the experimental chamber. The number of pulses administered was kept to the minimum necessary to produce a contraction with a stable “plateau” force, at which the response of the fiber to changes in cell length could be determined. For this reason, the temperature of our experiments was kept low (1°C), because at this temperature a single pulse induced a twitch response that approached the tetanic tension level. The total duration of the contraction was 400–500 ms. The combination of brief tetani and low temperature permitted us to extend the experiment over a long time period without unnecessary mechanical stress for the preparation. The fiber was exposed briefly to synchrotron radiation during the contractions, and the

Received for publication 8 October 1997 and in final form 16 July 1998.

Address reprint requests to Dr. P. J. Griffiths, University Laboratory of Physiology, Parks Road, Oxford OX1 3PT, England. Tel.: 441-865-272494; Fax: 441-865-272469; E-mail: pjg@physiol.ox.ac.uk.

© 1998 by the Biophysical Society

0006-3495/98/12/2984/12 \$2.00

equatorial x-ray diffraction pattern was sampled for 1 ms, and for a short period before activation (a single sampling of 30 ms), so that the relaxed equatorial pattern could also be recorded. The pattern was recorded on a one-dimensional multiwire detector with 128 channels, each collecting counts from a 1-mm region of the equatorial pattern (Hendrix et al., 1982). Sarcomere length was monitored throughout the experiment with a laser diffractometer system. During contraction, fibers were allowed to shorten at a velocity close to that of unloaded shortening (V_{\max}) and then to recover tension under isometric conditions. Data were archived to compact disks and subsequently analyzed with a selection of commercially available statistical and fitting routines (Press et al., 1989) running under Fortran (Salford Software, Salford, England). Lattice spacing (the center-to-center distance between adjacent myosin filaments) was determined from the center point of Gaussian functions fitted to the 10 and 11 reflections. Details of the beamline and data analysis have been published elsewhere (Cecchi et al., 1991).

The experimental protocol consisted of a period of repetitive tetanic stimuli (20 Hz) separated by rest intervals of between 20 s and 300 s. This regime was maintained over 100–200 tetani, then a recovery period of 1 h was permitted, during which the fiber was not stimulated, and the time course of the lattice spacing recovery was followed. In addition to obtaining the time course of slow changes in lattice spacing over the period of repetitive stimulation, this protocol also enabled us to obtain high time resolution data on dynamic lattice spacing changes during contraction, by summation of x-ray patterns from 10 to 20 contractions at a chosen degree of swelling. Although tetanic force declined by up to 40% at the shortest rest intervals, it was fully restored by the end of the recovery period. All experiments were conducted at the X-13 beamline in Hamburg, using the positron storage ring DORIS as the source of synchrotron radiation.

Simulations of osmolyte accumulation

The consequences of osmolyte accumulation in the sarcoplasm were estimated by computer simulation of the intracellular milieu. We assumed the concentrations of the principal chemical constituents of the cell to be as listed in Godt and Maughan (1988) and chose appropriate equilibrium constants for proton and metal binding from Martell and Smith (1974) and Sillén and Martell (1971). Because experiments were performed at 1°C, the van't Hoff isochore was used, where possible, to obtain equilibrium constants at this temperature, using the enthalpies of the reactions concerned; otherwise the affinities at 25°C were used. Protonation steps were corrected for ionic strength as outlined in Martell and Smith (1974). Lactate accumulation causes a release of protons, whereas phosphate accumulation leads to proton uptake. Therefore, to calculate the pH arrived at in a mixture of accumulated lactate and phosphate, the net production or absorption of protons was calculated for the accumulated metabolites at pH 7.18, and the total buffering capacity of the fiber was used to obtain a final pH value. The buffering power of a rested, relaxed fiber was taken as 37.3 mM/pH unit from Curtin (1986), whose experiments indicate that the buffering power deviates little from this value over a pH range of 6.4–7.4 in frog muscle. The buffering power (B) of a solution can be defined as the negative ratio of the quantity of protons added to the system divided by the change in pH. For each of n buffer species present in a system at a total concentration $[L_{\text{total}}]_i$ and with a proton dissociation constant K_i , we may write

$$[\text{HL}]_i = \frac{[L_{\text{total}}]_i [\text{H}^+]}{K_i + [\text{H}^+]}, \quad \frac{d[\text{HL}]_i}{d[\text{H}^+]} = \frac{K_i [L_{\text{total}}]_i}{(K_i + [\text{H}^+])^2}$$

and for water,

$$[\text{OH}^-] = \frac{K_w}{[\text{H}^+]}, \quad \frac{d[\text{OH}^-]}{d[\text{H}^+]} = \frac{-K_w}{[\text{H}^+]^2}$$

where K_w is the ionic product of water. Because the incremental addition of protons must equal the incremental change in $[\text{HL}]_i$ and $[\text{H}^+]$ minus the change in $[\text{OH}^-]$ (because negative changes in $[\text{OH}^-]$ indicate a positive

change in protons bound as H_2O), and noting that $\ln[\text{H}^+] = -\text{pH} \ln(10)$, and thus $d[\text{H}^+]/d\text{pH} = -[\text{H}^+] \ln(10)$, application of the chain rule gives

$$B = \ln(10) \left[\sum_{i=1}^n \frac{K_i [L_{\text{total}}]_i [\text{H}^+]}{(K_i + [\text{H}^+])^2} + [\text{H}^+] + \frac{K_w}{[\text{H}^+]} \right]$$

The accumulated phosphate therefore can be regarded as the addition of an $(n + 1)$ th buffer, which will increase the buffering power by an amount $K[\text{P}_i][\text{H}^+] \ln(10)/(K + [\text{H}^+])^2$, taking $[\text{P}_i]$ as the sum of the concentrations of monovalent and divalent additional accumulated free phosphate ions above resting levels, and K as the dissociation constant of proton binding to the divalent phosphate species. An iterative method was used to obtain a pH satisfying the amount of protons released and the buffering power of the relaxed fiber and the accumulated phosphate. An estimate of the creatine phosphate concentration was obtained by assuming the total releasable phosphate ($[\text{P}_i] = [\text{PCr}] + [\text{ATP}] + [\text{P}_i]$) to remain constant. The concentration of creatine phosphate may be obtained from the relation given in Table 4 for the phosphorylation of creatine as

$$[\text{PCr}] = \frac{[\text{Cr}][\text{ATP}]}{\beta[\text{ADP}]}$$

where $\beta = K[\text{H}^+]^\alpha$, $\alpha = 0.8$, $K = 1.66 \times 10^{-9} \text{ M}^{-1}$ (38°C; Veech et al., 1979), $[\text{C}_i]$ is total creatine concentration, $[\text{A}_i] = [\text{ATP}] + [\text{ADP}]$, and $[\text{P}_i]$ is the sum of the concentrations of all forms of inorganic phosphate. Therefore, it follows that

$$[\text{PCr}] = \frac{([\text{C}_i] - [\text{PCr}])([\text{P}_i] - [\text{PCr}] - [\text{P}_i])}{\beta([\text{A}_i] - [\text{P}_i] + [\text{PCr}] + [\text{P}_i])}$$

which, on grouping of terms, yields a quadratic dependent on $[\text{P}_i]$, with a solution

$$[\text{PCr}] = \frac{(\beta - 1)([\text{P}_i] - [\text{P}_i]) - [\text{C}_i] - \beta[\text{A}_i]}{2(\beta - 1)} + \frac{\sqrt{([\text{C}_i] + \beta[\text{A}_i] + (1 - \beta)([\text{P}_i] - [\text{P}_i])^2 + 4[\text{C}_i](\beta - 1))}}{2(\beta - 1)}$$

The corresponding $[\text{ATP}]$, deduced from the equation for $[\text{PCr}]$ in Table 4, is given by

$$[\text{ATP}] = \frac{\beta[\text{PCr}][\text{A}_i]}{[\text{C}_i] + (\beta - 1)[\text{PCr}]}$$

Evaluated in the range pH 6.4–7.4, for a fiber swollen by 13%, taking $[\text{C}_i] = 53.63 \text{ mM}$, $[\text{A}_i] = 5.49 \text{ mM}$, $[\text{P}_i] = 50.61 \text{ mM}$, and total $[\text{P}_i]$ 28 mM (based on the values quoted in Godt and Maughan (1988) for unswollen fibers), these equations show a maximum free $[\text{ADP}]$ of $\sim 6 \mu\text{M}$ (resting fiber ADP content is thought to be almost entirely in a protein-bound form), and therefore phosphate accumulation of up to 28 mM corresponds almost exactly to the disappearance of creatine phosphate, because $[\text{ATP}]$ falls by $6 \mu\text{M}$ at most. The composition of the sarcoplasm was then solved for the appropriate pH for a given mixture of accumulated phosphate and lactate, using the pH and creatine phosphate values arrived at from the considerations above and a modified version of an iterative computer program for the determination of species in a mixture of metal and ligand ions (Perrin and Sayce, 1967).

RESULTS

The lattice spacing of the relaxed fiber, measured during the rest intervals, was found to increase during a period of repetitive stimulation at a rate determined by the duration of the rest intervals. Fig. 1 shows the change in spacing during

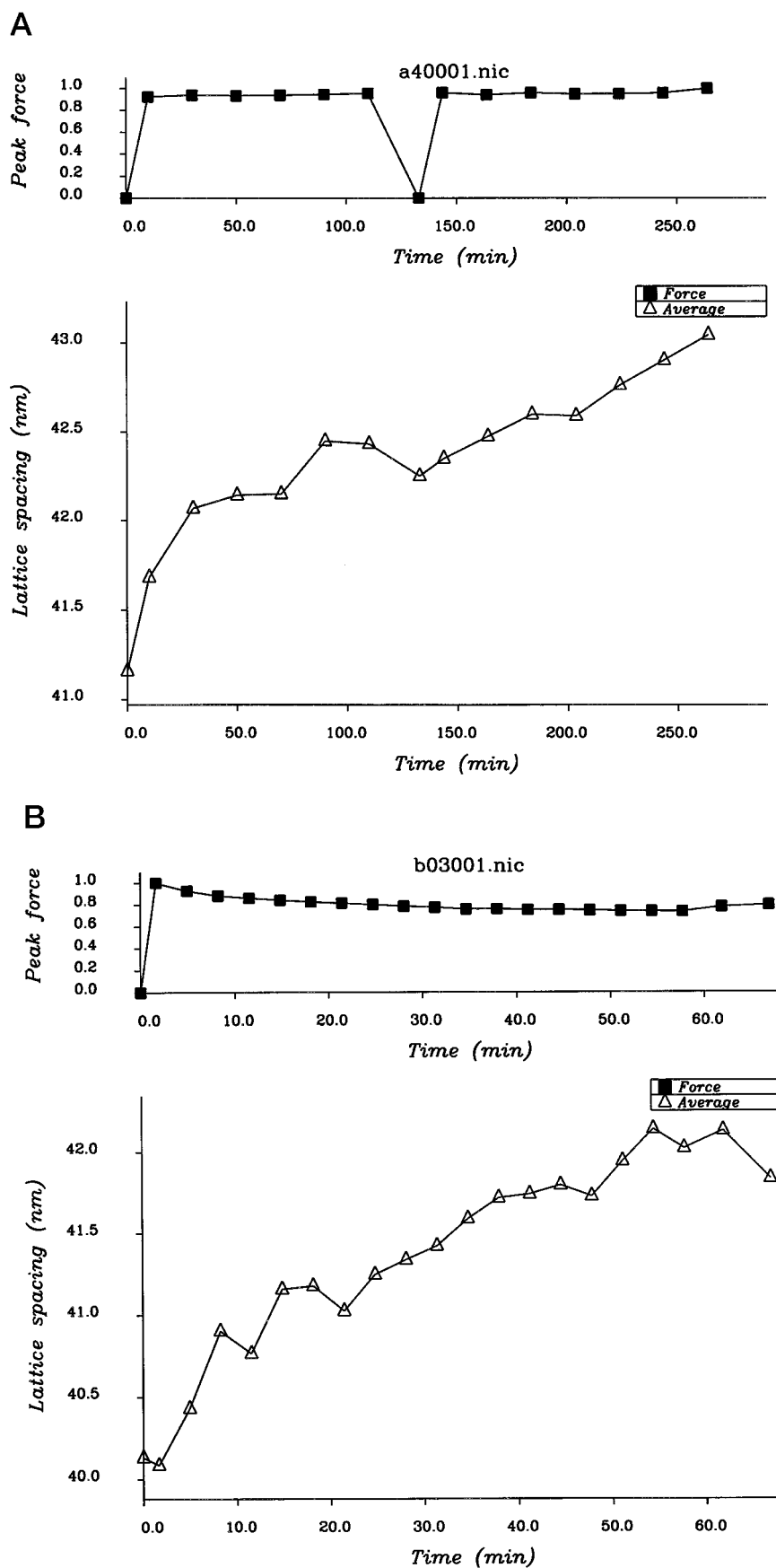


FIGURE 1 Lattice spacing (Δ) and peak tension (\blacksquare) for stimulation periods with rest intervals of 120 s (*top panels*) and 20 s (*bottom panels*). Both force and spacing data were obtained by summation of 10 cycles; hence points on the top panels occur every 20 min, and those on the lower panel every 3 min 20 s. The zero tension point in *A* at 130 min was due to positron injection into the synchrotron storage ring, during which stimulation was stopped. To show that stimulation was not continuous and to indicate the restart of the experiment, the tension has been set to zero.

a stimulation period with a rest interval of 120 s (*top panel*) and during a period with a rest interval of 20 s (*bottom panel*), with the accompanying values of peak tension normalized to its amplitude at the start of the stimulation period. For the longer rest period, spacing increased at a high rate initially up to $\sim 3.5\%$, but entered a period of more gradual expansion after 20 min. The peak force during the stimulation period remained stable throughout. For the shorter rest interval, an initial fast increase in spacing was also detectable. Beyond 10 min into the stimulation period, spacing increased more slowly, approaching a steady rate, whereas peak force declined slightly (8%).

The swelling of the lattice did not continue indefinitely when the period of stimulation was prolonged, but converged on a maximum spacing beyond which further expansion did not occur, even though stimulation and tension development continued. An example of this is shown in Fig. 2. For this fiber, lattice spacing was increased by repetitive stimulation with a 20-s rest interval. This fiber maintained a rapid lattice expansion beyond the initial rapid increase in spacing. It can be seen that expansion leveled off above 46 nm to become stable throughout the rest of the stimulation period. There was also a suppression of force to 70% of its initial value.

In Fig. 3, the recovery of lattice spacing on termination of the excitation period is shown. After 55 min of repetitive stimulation with a 20-s rest interval, the rest interval was increased to 300 s. The spacing changes are clearly divisible into three sections, the first two corresponding to the rapid

(phase 1) and slower (phase 2) periods of expansion during the excitation period, described above; the third, a gradual recovery of the initial spacing over a 60-min recovery period, occurred during the period when the rest interval had been increased to 300 s. When the restoration of the original spacing was complete, a new stimulation period resulted in a period of lattice expansion indistinguishable from the first (data not shown), showing that the expansion and recompression of the lattice are entirely reversible. Because all three phases appear to approximate to linear changes in spacing occurring at differing but constant rates, for simplicity we chose to fit each of them with a linear regression of spacing upon time. The best fit lines are shown on the figure, and the values of the rates for each phase are given in Table 1 for seven fibers in which all three rates could be determined. From Figs. 1–3 it can be seen that the principal reduction of the force response amplitude coincides with phase 1 and remains relatively stable during phase 2. On termination of the stimulation period, the force response underwent a gradual recovery similar to that of lattice spacing. When such a stimulation protocol was followed in the absence of x-ray exposure over a period of 2 h, and lattice spacing was determined from a single 0.5-s exposure to x-rays at the end of this period, the same increase in lattice volume was detected, as was subsequently the same recovery rate to the original spacing as in fibers exposed to x-rays throughout the stimulation period. Thus the expansion and recovery of lattice spacing are not the effects of

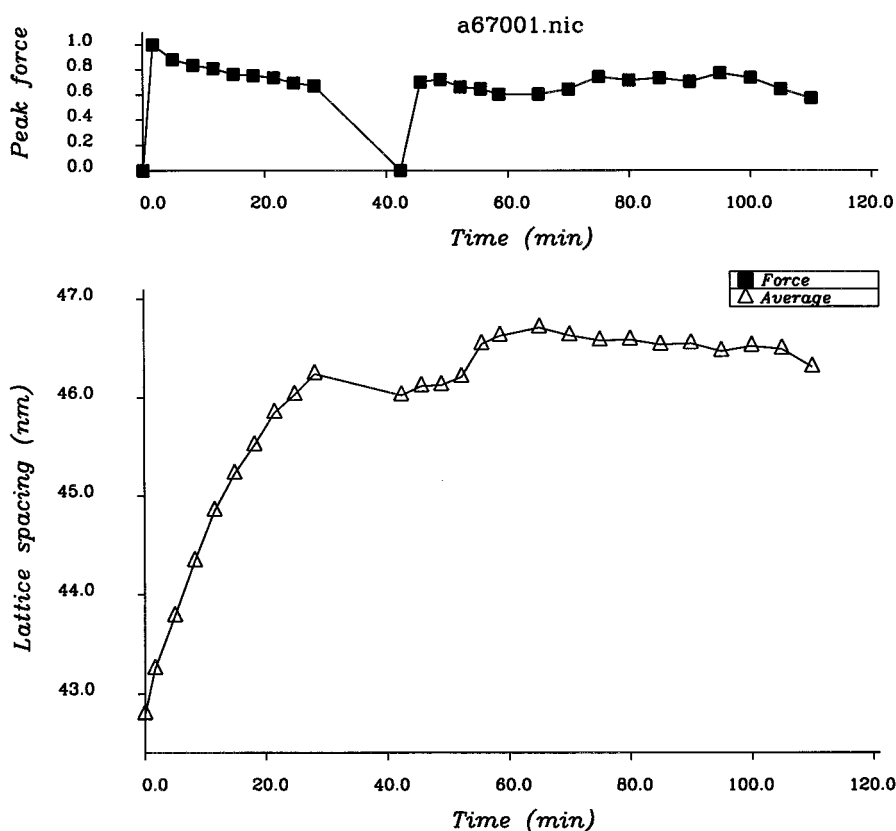


FIGURE 2 Lattice spacing and peak force as in Fig. 1. Once again, an injection of positrons interrupted the beam run and the stimulation was stopped. Therefore a brief period of spacing recovery began at 30 min, as indicated by the zero peak force value, before the experiment was restarted. Fluctuations on the tension trace are the result of small electrical offset adjustments on the force transducer to compensate for drift. Symbols are as for Fig. 1.

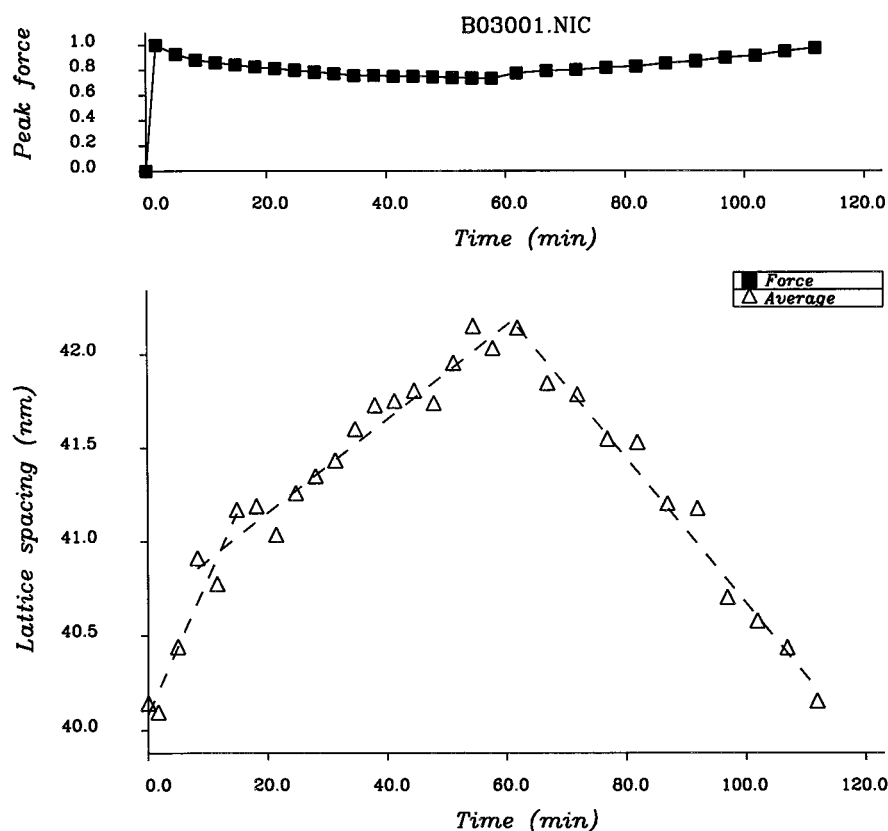


FIGURE 3 Lattice spacing and peak tension during the two phases of lattice expansion and the recovery phase. The rest period is 20 s. Dashed lines represent a least-squares fit to a linear regression for the data points over that range of time. Symbols are as for Fig. 1.

x-ray exposure manifested over a long time period of repetitive stimulation.

In Table 2 we show the rates of lattice expansion at different resting intervals for phases 1 and 2, expressing the rates either as per unit time or per contraction. For longer rest intervals, the duration of the experiment was much prolonged, and therefore we performed fewer experiments of this kind. It can be seen that when the rate of expansion is expressed in nanometers per minute, phase 1 expansion rate is clearly very dependent on the rest interval duration. However, when the rate of expansion during this phase is expressed as nanometers per contraction, the dependence on rest interval duration almost vanishes. This suggests that the processes that restore the original spacing during the recovery period occur at a very slow rate during phase 1, and therefore the contribution to expansion by each contraction is not reduced as the rest interval duration increases. In the

case of phase 2, the rate of expansion per minute is also dependent on rest interval duration, although less markedly so, and the rate of expansion per contraction now also shows some sensitivity to rest interval duration. This suggests that the recovery processes are now proceeding at a higher rate, in agreement with the values given in Table 1, which show the recovery rate to be equal to or larger than the expansion rate during phase 2.

Lattice spacing of the relaxed fiber is sensitive to sarcomere length changes because of the constraints of maintenance of constant volume. Thus the changes in spacing we have observed could arise from a change in fiber length during the course of an experiment. Therefore we adjusted the measured values of lattice spacing for the sarcomere length of the fiber, which was monitored continuously throughout the experiment, by multiplication of the observed spacing by the square root of the ratio of sarcomere length at that point during the experiment to the sarcomere length at the start of the experiment. The behavior of sarcomere length during the stimulation period was not consistent, but usually it decreased steadily throughout the stimulation period. However, the total sarcomere length change was small and did not affect the rates of expansion greatly or the decline in force. For example, for the shortest resting period, during which the number of fibers examined was largest and so less susceptible to statistical fluctuation, the mean values of expansion rates for phases 1 and 2 were 0.132 and 0.044 nm/min, respectively. Correction for sarcomere length changes adjusted these values to 0.125 and

TABLE 1 Expansion and recovery rates for seven fibers in which all three phases could be detected

Fiber number	Phase 1 (nm · min ⁻¹)	Phase 2 (nm · min ⁻¹)	Recovery phase (nm · min ⁻¹)
A31	0.098	0.035	0.028
B03	0.075	0.025	0.039
B38	0.129	0.032	0.059
F29	0.085	0.024	0.040
F40	0.069	0.031	0.060
F77	0.025	0.005	0.022
F91	0.108	0.010	0.094

TABLE 2 Rates of expansion of the lattice during repetitive stimulation

Rest time (s)	Phase 1 rate (nm · min ⁻¹)	Phase 1 rate (nm/contraction)	Phase 2 rate (nm · min ⁻¹)	Phase 2 rate (nm/contraction)	<i>N</i>	Δx per contraction ($\mu\text{mol} \cdot \text{liter}^{-1}$)
20	0.132 ± 0.028	0.044 ± 0.010	0.044 ± 0.019	0.015 ± 0.006	8	527 ± 164
25	0.094 ± 0.014	0.039 ± 0.010	0.033 ± 0.028	0.013 ± 0.011	4	447 ± 110
40	0.069	0.049	0.021	0.015	1	558
60	0.059	0.035	0.050	0.059	1	395
90	0.023	0.034	0.011	0.016	1	384
120	0.025	0.047	0.005	0.010	2	520
180	0.012	0.037	0.002	0.005	2	407
300	—	—	0.002	0.008	2	—

Because the timing of contractions was sometimes interrupted by adjustments to the beam or the fiber position, the number of contractions given over a particular time period differed from that expected from the rest interval, and so the expansion per contraction in columns 3 and 5 often differs a little from the expected value based on columns 2 and 4. Values of Δx were computed from the phase 1 expansion rate per minute and the lattice spacing of the cells at the start of the stimulation period, using Eq. 1. Because of variation in the rested relaxed lattice spacing at the start of the experiment, the ratios of these values differ a little from the ratios of the corresponding values in column 3.

0.047 nm/min, which is only a ~5% adjustment of the expansion rates observed. In Table 3 we show the values of expansion rates per unit time for phases 1 and 2 before and after correction for sarcomere length changes.

The most likely reason for the expansion of the lattice reported here is the production of osmolytes as a result of elevated rates of ATP hydrolysis and synthesis due to mechanical activity. In our previous studies, we have found that the recovery of isometric tension after a period of unloaded shortening is accompanied by a compression of the A band lattice and that this compression was increased when the lattice was expanded by exposure of the muscle fiber to hypotonic conditions (Bagni et al., 1994). It was therefore of interest to observe the effect lattice swelling due to repetitive stimulation had on this lattice compression, because, in the present experiments, the bathing medium tonicity was unaltered. The force responses to electrical stimulation and to shortening at a velocity approaching V_{\max} , obtained from a fiber before and after the swelling of the lattice, are shown in Fig. 4. In the left panel of Fig. 4, the lattice spacing can be seen to increase rapidly from 42.75 nm at the onset of shortening (i.e., at the abrupt fall in tension), then to be recompressed during the isometric redevelopment of tension after the shortening. In the right panel, the same fiber has been allowed to shorten in the same manner, but after expansion of the lattice to 45.1 nm by repetitive stimulation. It can be seen that the isometric recompression of the lattice after shortening is larger than in the unexpanded lattice. The recompression of the lattice after a period of shortening at V_{\max} was fitted to an exponential function, and the amplitude of the compression phase was obtained. In six fibers examined before swelling (lattice spacing 42.11 nm), the recompression amplitude was 0.689 ± 0.122 nm. After swelling (spacing 44.74 nm), the recompression amplitude increased to 1.521 ± 0.106 nm. Therefore, although the axial tension was reduced in fibers with a lattice swollen by up to 30%, the changes in lattice spacing that accompany contraction and force redevelopment became more pronounced. The apparent rate constant for the recompression in the control fibers was

$17.4 \pm 6.1 \text{ s}^{-1}$. In the swollen lattice we obtained a value of $15.9 \pm 5.1 \text{ s}^{-1}$, suggesting that the kinetics of the lattice compression were slowed slightly by the swelling of the fiber.

The effects of osmolyte accumulation on the sarcoplasm were estimated from the concentrations of the principal ions present in the sarcoplasm and their stability constants, using a treatment similar to that of Godt and Maughan (1988). Like these authors, we also assumed an intracellular pH in resting fibers of 7.18 but chose a free $[\text{Mg}^{2+}]$ of 1.0 mM and a free $[\text{Ca}^{2+}]$ of 0.1 μM ; otherwise concentrations and equilibrium constants used were similar to those of Godt and Maughan (1988). In the six swollen fibers from which time-resolved lattice spacing data were obtained, the mean volume increase was 13%, corresponding to a production of 26.46 mM osmolyte. In Fig. 5 we have plotted the expected change in pH and ionic strength for this quantity of osmolyte against percentage of phosphate in the accumulated osmolyte; the remaining osmolyte was assumed to be lactate. Table 4 lists in detail the principal ionic species in the sarcoplasm for phosphate or lactate accumulation and the concentrations of their complexes with metal ions. It is apparent that when less than 83% of the accumulated os-

TABLE 3 Rates of expansion per unit time for phases 1 and 2

Rest time (s)	Phase 1 rate (nm · min ⁻¹) uncorrected	Phase 1 rate (nm · min ⁻¹) corrected	Phase 2 rate (nm · min ⁻¹) uncorrected	Phase 2 rate (nm · min ⁻¹) corrected
20	0.132 ± 0.028	0.125 ± 0.029	0.044 ± 0.019	0.047 ± 0.006
25	0.094 ± 0.014	0.091 ± 0.035	0.033 ± 0.028	0.023 ± 0.008
40	0.069	0.095	0.021	0.025
60	0.059	0.073	0.050	0.018
90	0.023	0.021	0.011	0.011
180	0.012	0.009	0.002	0.000
300	—	—	0.002	0.001

Uncorrected values are the observed rates; corrected values have been adjusted for the sarcomere length at the time of the measurement compared to that at the start of the experiment, assuming that constant volume relations are maintained in the swollen lattice.

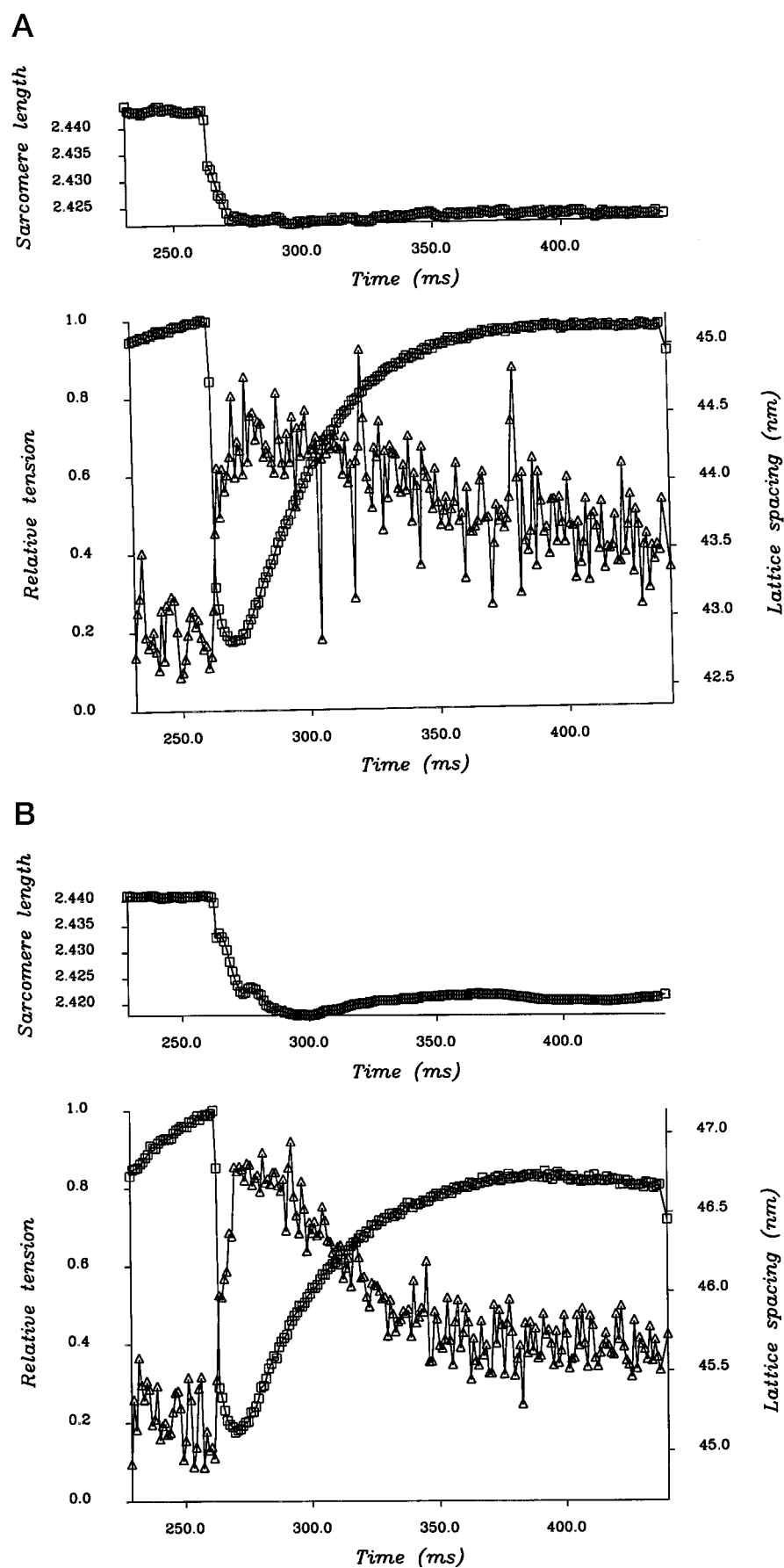
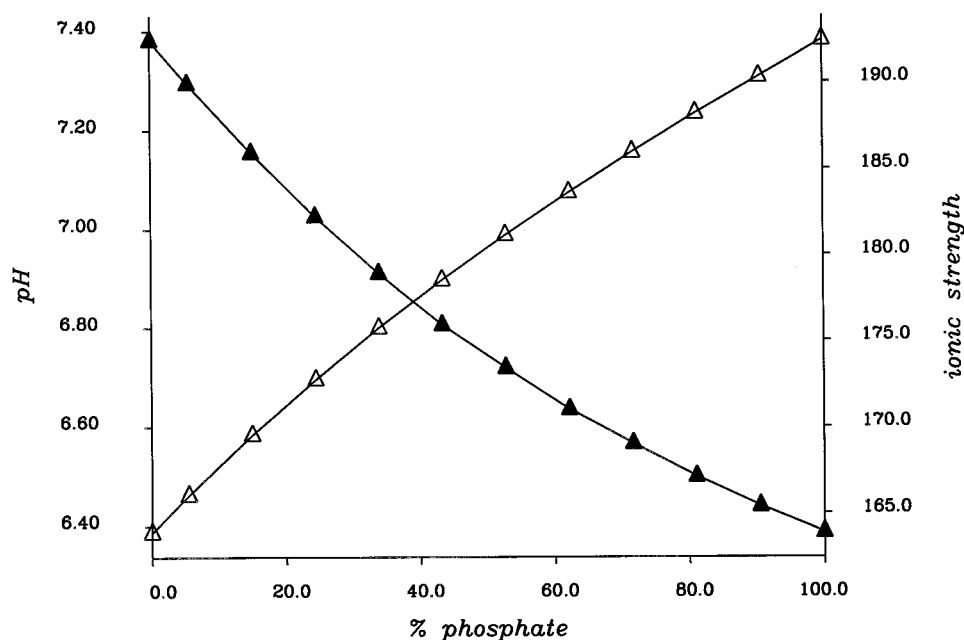


FIGURE 4 Lattice spacing changes during and after a period of shortening at close to V_{\max} imposed at the tetanic plateau in a fiber at its normal lattice spacing and subsequently at an expanded lattice spacing after repetitive stimulation. (A) Lattice spacing changes, force, and sarcomere length in the unexpanded lattice. (B) The same parameters after repetitive stimulation with a 20-s rest interval over 1 h.

FIGURE 5 Intracellular ionic strength (\blacktriangle , mM) and pH (\triangle) as a function of % $[P_i]$ in a solution simulating the composition of sarco-plasm in which 26.46 mM metabolite has accumulated. The metabolite is assumed to be composed of a mixture of phosphate and lactate (i.e., 10% phosphate indicates $[P_i] = 2.646$ mM + resting fiber $[P_i]$, $[\text{lactate}] = 23.814$ + resting fiber $[\text{lactate}]$). The resting fiber concentrations were obtained from Godt and Maughan (1988) and corrected for an increase in fiber volume of 13%.



molyte is phosphate, acidification of the fiber results, whereas phosphate accumulation greater than 83% of the total accumulated osmolyte caused the fiber to become more alkaline. The ionic strength computed for a rested relaxed fiber was 195 mM; therefore ionic strength is expected to have fallen in swollen fibers for all phosphate/lactate ratios, although the fall is only 3.3% when the osmolyte produced is predominantly lactate.

DISCUSSION

Relation between rate of osmolyte accumulation and spacing changes

During repetitive, brief stimulation, A band lattice spacing of an intact skeletal muscle fiber increased at a rate determined by the rest interval between contractions. On termination of the stimulation period, spacing recovered over a period of 60 min at 1°C. Because the extramyofibrillar space into which the lattice might be able to expand is too small to account for the expansion (17% of fiber volume; Mobley and Eisenberg, 1975), this must indicate a change in cell volume. An increase in fiber volume of up to 35% during stimulation to fatigue has been reported in intact *Xenopus* fibers (Lännergren, 1990). The forces required to cause such an increase in cell volume are too large for a mechanical or electrostatic origin (Schoenberg, 1980) but could arise from an osmotic pressure change associated with mechanical activity. Taking the tension in the cell membrane to be very small and assuming fiber tonicity remains constant during the stimulation period, for small changes of lattice spacing we may relate the relative spacing change to the relative change in internal osmolyte quantity and to the rate of osmolyte production according to the following simple relations. Let x_0 and a_0 be the initial quantity of

osmolytes inside the fiber and the initial lattice spacing, and let Δx and Δa indicate the change in these quantities as a result of stimulation. A quantity of osmolyte material produced, Δx , causes a change in volume, Δv , having the relation $\Delta x/x_0 = \Delta v/v_0$. Because volume is proportional to spacing squared, if osmolyte pressure remains in equilibrium across the membrane, then it follows that

$$\frac{x_0 + \Delta x}{x_0} = \frac{(a_0 + \Delta a)^2}{a_0^2}$$

Therefore, taking initial tonicity as c_0 , change in osmolyte quantity or concentration is

$$\frac{\Delta x}{x_0} = \frac{2a_0\Delta a + (\Delta a)^2}{a_0^2}, \quad \Delta c = \frac{\Delta x}{v_0 + \Delta v} = \frac{c_0\Delta v}{v_0 + \Delta v}$$

so, if Δa is small compared to a_0 , this relation may be simplified to that of Eq. 1:

$$\frac{\Delta x}{x_0} \approx \frac{2\Delta a}{a_0} \quad (1)$$

$$a(t) = a_0 + kt - \alpha t \quad (2)$$

$$\frac{d}{dt}\left(\frac{\Delta x}{x_0}\right) \approx 2\frac{d}{dt}\left(\frac{\Delta a}{a_0}\right) = \frac{2(k - \alpha)}{a_0} \quad (3)$$

Equation 2 represents the spacing change as a balance between the rate of increase in lattice spacing as a result of production of osmolyte (k) and the rate of decrease due to its removal (α). Substituting $(a_0 + \Delta a)$ for $a(t)$ and normalizing to initial spacing, the differential of Eq. 2 yields the net rate of change of quantity of osmolyte (Eq. 3).

TABLE 4 Principal ionic, sarcoplasmic species concentrations, calculated for 26.46 mM phosphate accumulation, $[A^-] = 44.19$ mM, pH 7.392 (solution A), and 26.46 mM lactate accumulation, $[A^-] = 22.49$ mM, pH 6.386 (solution B), using $[Ca^{2+}] = 0.1 \mu\text{M}$, $[Mg]_{\text{total}} = 7.5 \text{ mM}$, $[Na]_{\text{total}} = 8 \text{ mM}$, $[K]_{\text{total}} = 125 \text{ mM}$

Species	$\log K$ 1°C $\Gamma = 0.2\text{M}$	Reaction	Concentration solution A (M)	Concentration solution B (M)	Enthalpy (kJ · mol ⁻¹)
ATP ⁴⁻		[L]	4.87×10^{-4}	3.88×10^{-4}	
HATP ³⁻	6.67	[HL]/[H][L]	9.30×10^{-5}	7.52×10^{-4}	-0.84
H ₂ ATP ²⁻	4.41	[H ₂ L]/[H][HL]	9.73×10^{-8}	7.98×10^{-6}	-15.06
MgATP ²⁻	3.97	[ML]/[M][L]	4.33×10^{-3}	3.78×10^{-3}	18.83
CaATP ²⁻	4.02	[ML]/[M][L]	5.48×10^{-7}	4.78×10^{-7}	-4.184
MgHATP ⁻	2.11	[MHL]/[H][ML]	1.14×10^{-5}	1.01×10^{-4}	8.368
CaHATP ⁻	2.13	[MHL]/[H][ML]	1.33×10^{-9}	1.18×10^{-8}	0.00
KATP ³⁻	0.93	[ML]/[M][L]	5.06×10^{-4}	4.12×10^{-4}	1.26
NaATP ³⁻	1.12	[ML]/[M][L]	5.01×10^{-5}	4.08×10^{-5}	-0.84
ADP ³⁻		[L]	1.85×10^{-6}	2.19×10^{-8}	
HADP ²⁻	6.56	[HL]/[H][L]	2.76×10^{-7}	3.31×10^{-8}	-2.93
H ₂ ADP ⁻	4.33	[H ₂ L]/[H][HL]	2.41×10^{-10}	2.94×10^{-10}	-17.15
MgADP ⁻	3.02	[ML]/[M][L]	1.86×10^{-6}	2.42×10^{-8}	13.39
CaADP ⁻	2.94	[ML]/[M][L]	1.73×10^{-10}	2.24×10^{-12}	-4.184
MgHADP	1.54	[MHL]/[H][ML]	9.21×10^{-9}	1.21×10^{-9}	4.184
CaHADP	1.58	[MHL]/[H][ML]	1.11×10^{-12}	1.46×10^{-13}	0.00
KADP ²⁻	0.82	[ML]/[M][L]	1.49×10^{-6}	1.80×10^{-8}	
NaADP ²⁻	0.89	[ML]/[M][L]	1.11×10^{-7}	1.35×10^{-9}	
PO ₃ ³⁻		[L]	2.85×10^{-7}	3.71×10^{-10}	
HPO ₃ ²⁻	12.19	[HL]/[H][L]	1.79×10^{-2}	2.36×10^{-4}	-17.57
H ₂ PO ₃ ⁻	6.95	[H ₂ L]/[H][HL]	6.48×10^{-3}	8.68×10^{-4}	-4.6
H ₃ PO ₃	1.89	[H ₃ L]/[H][H ₂ L]	2.06×10^{-8}	2.80×10^{-8}	8.79
CaPO ₃ ⁻	6.27	[ML]/[M][L]	5.60×10^{-8}	7.98×10^{-11}	12.55
MgPO ₃ ⁻	3.40	[ML]/[M][L]	6.80×10^{-7}	9.72×10^{-10}	
CaHPO ₃	1.31	[MHL]/[M][HL]	3.86×10^{-8}	5.58×10^{-10}	12.55
MgHPO ₃	1.67	[MHL]/[M][HL]	4.35×10^{-5}	1.16×10^{-5}	12.13
KPO ₃ ²⁻	0.15	[ML]/[M][L]	4.95×10^{-8}	6.57×10^{-11}	25.104
NaPO ₃ ²⁻	0.30	[ML]/[M][L]	4.45×10^{-9}	5.93×10^{-12}	33.472
KHPO ₃ ⁻	-0.10	[MHL]/[M][HL]	1.73×10^{-3}	2.33×10^{-5}	29.29
NaHPO ₃ ⁻	-0.02	[MHL]/[M][HL]	1.31×10^{-4}	1.77×10^{-6}	33.47
KH ₂ PO ₃	-0.14	[MH ₂ L]/[M][H ₂ L]	5.71×10^{-4}	7.79×10^{-5}	
NaH ₂ PO ₃	-0.14	[MH ₂ L]/[M][H ₂ L]	3.63×10^{-5}	4.96×10^{-6}	
Cr		—	9.73×10^{-3}	9.73×10^{-3}	
PCr ²⁻	9.22	[Cr][ATP]/ [PCr][ADP][H] ^{0.8}	1.68×10^{-2}	4.13×10^{-2}	
MgPCr	1.6	[MHL]/[M][HL]	6.35×10^{-4}	1.72×10^{-3}	
CaPCr	1.3	[MHL]/[M][HL]	3.56×10^{-8}	9.59×10^{-8}	
Lactate ⁻		[L]	1.32×10^{-3}	2.75×10^{-2}	
HLactate	3.78	[HL]/[H][L]	3.25×10^{-7}	6.88×10^{-5}	0.33
MgLactate ⁺	0.93	[ML]/[M][L]	1.07×10^{-5}	2.44×10^{-4}	
CaLactate ⁺	1.07	[ML]/[M][L]	1.64×10^{-9}	3.76×10^{-8}	
Carnosine		[HL]	1.30×10^{-2}	4.12×10^{-3}	
HCarnosine ⁺	6.89	[H ₂ L]/[H][HL]	4.08×10^{-3}	1.31×10^{-2}	
MgCarnosine ⁺	3.10	[ML]/[M][L]	1.27×10^{-4}	4.35×10^{-6}	
CaCarnosine ⁺	3.22	[ML]/[M][L]	1.87×10^{-8}	6.40×10^{-10}	
PV1 ²⁻		[L]	2.22×10^{-7}	2.03×10^{-7}	
MgPV1	6.21	[ML]/[M][L]	3.42×10^{-4}	3.42×10^{-4}	-33.0
CaPV1	10.36	[ML]/[M][L]	5.43×10^{-4}	5.43×10^{-4}	-56.0
PV2 ²⁻		[L]	1.22×10^{-5}	1.12×10^{-5}	
MgPV2	4.36	[ML]/[M][L]	2.67×10^{-4}	2.68×10^{-4}	9.0
CaPV2	8.67	[ML]/[M][L]	6.06×10^{-4}	6.06×10^{-4}	-24.0

$[A^-]$ is the charge deficit obtained from the sum of total charge accounted for by the species above, and represents principally fixed charges (plus a small contribution from amino acids, soluble proteins, glycolytic intermediates, and $[Cl^-]$ ions; see Godt and Maughan, 1988). PV1 and PV2 are the two parvalbumin divalent cation binding sites, which are treated as independent sites. $[ADP]_{\text{total}}$ is taken as free ADP, the majority of ADP in the cell being in a bound state, and assumed not to participate in metal ion binding. Log K values are the actual constants used in the calculations (i.e., adjusted for proton activity and temperature). Data were taken from Martell and Smith (1974), Sillén and Martell (1971), Veech et al. (1979), Dawson et al. (1979), and Tanokura et al. (1986).

Origin of osmolyte production

In Table 2, the rate of expansion of the lattice for phases 1 and 2 has been calculated per contraction, and for phase 1 as the quantity of osmolyte produced, using Eq. 3. Although the rate of production of osmolyte per unit time during phase 1 was very sensitive to rest interval duration, the expansion per contraction was almost constant at 0.04 nm per contraction, or 0.45 mOsmol/liter of fiber per contraction (taking x_0 as 230 mOsmol/liter, the osmolarity of Ringer's solution) from Eq. 3. The influx of monovalent cations during an action potential is small (only $\sim 6 \mu\text{Osmol/liter}$ of fiber per action potential; Kushmerick, 1983) and largely balanced by potassium efflux, so we believe the osmotically active material to originate from activity of the contractile machinery and the sarcoplasmic reticulum (sarcoplasmic reticulum ATPase accounting for 25–30% of the total ATPase activity during isometric contractions; Kushmerick, 1983) and not ionic currents. Fibers used in these experiments were selected for large size, so they may be assumed to be strongly dependent on glycolysis for ATP production, at least in the early stages of the stimulation period (because the large volume-to-surface area ratio would limit oxygen availability for oxidative ATP regeneration), where glycolysis contributes 80% of ATP production in the prefatigue condition in *Xenopus* muscle (Nagesser et al., 1993). For three ATP molecules regenerated by glycolysis, two molecules of lactic acid are produced, to which the cell membrane is weakly permeant and which could therefore cause fiber swelling. Both inorganic phosphate and lactate levels rise significantly after contraction. Phosphate is restored to its resting level with a half-time on the order of 10 min by glycolysis (4°C; Dawson et al., 1977), and lactate levels are restored by efflux through the cell membrane, either via a lactate-proton cotransporter or by passive diffusion (principally of undissociated lactic acid), with a half-time of ~ 20 min in *Xenopus laevis* at 20°C (Nagesser et al., 1994). Restoration of lattice spacing upon termination of stimulation occurred over a period of 60 min (mean $\alpha = 0.049 \text{ nm} \cdot \text{min}^{-1}$), which, given the low temperature of our experiments, is consistent with the reported removal rates of both metabolites.

Origin of the two phases of lattice expansion

The constancy of the expansion per contraction during phase 1 irrespective of rest interval suggests that α is much smaller during this phase. This is because the spacing change per contraction with a 20-s rest interval would depend on osmolyte production minus the recompression expected for a 20-s recovery. A rest interval of 120 s would provide a sixfold longer period in which the lattice should recompress at the rate α , and so the expansion per contraction should be much reduced, yet this is not what is observed. In addition, Nagesser et al. (1993), using an experimental protocol similar to that used here, showed that the accumulation of lactic acid and inorganic phosphate in

Xenopus muscle starts at a high rate but declines rapidly in the first 5 min of a stimulation period, then remains stable. The absence of further lactate accumulation is due to a reduction in the rate of glycolysis, which is balanced by a fall in ATP hydrolysis rate by the contractile apparatus. Given the lower temperature of our experiments and our less taxing stimulation regime, it seems likely that our two phases of lattice expansion could arise from a similar adjustment in phosphate and lactate accumulation rates. Phases 1 and 2 do not arise from a reduction in sarcomere length during the early part of the stimulation period, as shown in Table 3, where we have corrected the expansion phases for changes in lattice spacing due to preparation shortening. As the effect of this correction is small (typically a 5% reduction in rate per contraction) and was not possible in all fibers, throughout the discussion we will continue to consider only the uncorrected expansion rates. From Table 1 it may be seen that the rate of phase 2 is similar to the difference between the rates of phase 1 and the recovery rate. If phase 1 arose from an initially small recovery rate (α) and phase 2 from a delayed increase of α , then phase 2 would appear as the difference between k and α . The rate of phase 1 expressed per contraction in Table 1 is similar to the measured ATPase activity in frog muscle at 0°C ($0.4 \mu\text{mol} \cdot \text{g}^{-1} \cdot \text{s}^{-1}$; Curtin et al., 1974) and is independent of rest interval, supporting the idea that α may be very small during this phase. The phase 1 expansion rate expressed per unit time in Table 2 is more clearly dependent on the rest interval duration than is the phase 2 rate. This may be because α is variable, depending on the degree of product accumulation. It must be noted that because phase 1 is relatively rapid and its form is not well defined, it may represent an exponential approach to a steady rate of expansion. In that event, its initial rate in the absence of significant recovery would be substantially higher than our estimates based on a simple linear expansion.

Lattice expansion has a "limiting spacing"

The expansion of the lattice during the stimulation period does not continue indefinitely, but reaches a maximum between 46 and 47 nm. This "limiting spacing" may arise from the same mechanical constraints that ultimately limit lattice expansion after skinning (Matsubara and Elliott, 1972) and need not correspond to a limiting volume of the cell. Hence further accumulation of metabolites may continue to increase cell volume not occupied by myofibrils. A similar conclusion was reached by April et al. (1972) from experiments performed on crayfish muscle. This may explain why Lännergren (1990) was able to observe a larger cell volume increase on fatigue than reported here. Taking the tonicity of the extracellular medium as 230 mM, a change in cell volume of 20% (the largest change in lattice volume detected here) suggests a production of 38 mOsmol $\cdot \text{liter}^{-1}$ osmolytes. Consumption of creatine phosphate alone is sufficient to reach this concentration of os-

molyte (e.g., 37 mmol inorganic phosphate/liter of fiber in Nagesser et al., 1993). Such an accumulation of phosphate would explain the force depression that accompanies lattice swelling in our experiments. If the osmolyte that accumulates were principally lactate, then the fall in pH associated with the build-up of this compound could reduce force by affecting calcium activation (Lee et al., 1991). In some experiments, substantial swelling was observed without change in tension, showing that accumulation of osmolytes can be undetected by force measurements. In experiments requiring repetitive stimulation of the muscle, this accumulation could be of importance, and we suggest that brief tetani should not be applied more frequently than one contraction every 3 min if this accumulation is to be minimized.

Relation to dynamic lattice spacing changes in intact cells at altered medium tonicity

Accumulation of phosphate or lactate would result in a reduction of force similar to that observed here: phosphate by direct action on contraction and regulation (20% reduction in maximum force in 10 mM phosphate; Godt and Nosek, 1989), lactate by the accompanying acidification, which reduces both the calcium sensitivity of thin filament regulation and the maximum calcium activated force (~50% reduction for one pH unit acidification; Godt and Nosek, 1989). The release of calcium ions from the sarcoplasmic reticulum upon activation seems relatively insensitive to pH (evidence summarized in Allen et al., 1995).

For an increase in volume of 13% (mean swelling for six fibers in which its effect on the time course of lattice recompression after shortening was studied), an accumulation of 26.46 mM of osmolyte would be expected. The lattice spacing changes associated with activation in these fibers were enhanced, particularly the lattice compression associated with the recovery of axial tension after a period of isotonic shortening. This observation is in agreement with that of Bagni et al. (1994), who used hypotonicity to expand the lattice of a single fiber. In the unswollen lattice, we obtained a compression value of 0.689 nm, and for the swollen lattice we have a value of 1.521 nm, similar to that reported by Bagni et al. (1994), who found 0.771 nm compression in control fibers and 1.703 nm in hypotonic saline (spacing 44.88 nm). In addition, axial force was reduced by 30% in the expanded fiber experiments reported here, whereas hypotonicity increased axial force by 11.7% in the experiments of Bagni et al. (1994). If radial and axial forces were affected in similar ways by the accumulation of metabolites, then radial force could have been reduced to 63% of its value under hypotonic conditions at the corresponding spacing.

From our considerations of the creatine phosphate equilibrium with ATP, [ATP] may be taken to be the same in both the swollen fibers used here and those exposed to hypotonicity by Bagni et al. (1994). The similarity of the radial force behavior in both types of expanded lattice

further suggests that the accumulation of metabolites, change in intracellular tonicity, and pH change have little effect on radial force development beyond that manifest in the axial force response. The sum of the charges of all species in the simulated sarcoplasm yields a negative charge deficit, which represents chiefly the fixed charges associated with the myofilaments (Godt and Maughan, 1988). Depending on the phosphate-to-lactate ratio of the accumulated metabolites, in fibers swollen by 13% this may vary from an increase in negative charge of 12% to a decrease of 43%, depending on the intracellular pH. Therefore, unless pH remains unchanged in the swollen fibers, radial forces appear not to be greatly sensitive to changes in these fixed charges. In the case of ionic strength, a fiber swollen to 1.13 times its original volume in hypotonic saline would be expected to have an ionic strength of 173 mM. The ionic strength of fibers swollen by metabolite accumulation would depend on the phosphate-to-lactate ratio, but because accumulations of lactate and phosphate appear to proceed at similar rates in amphibian muscle (Nagesser et al., 1993), it seems likely that their ratio in swollen fibers is close to unity. From Fig. 5 the intracellular ionic strength would be expected to be ~168 mM, based on the constants and reactions given in Table 4, somewhat lower than in fibers in hypotonic saline; therefore a contribution to the enhancement of radial forces from the reduction of ionic strength cannot be convincingly rejected, but because a similar enhancement of radial forces at constant ionic strength is observed in skinned muscle fibers at increased lattice spacing (Brenner and Yu, 1991), this argues strongly for spacing acting as the dominant factor. Therefore, these findings are consistent with the view that the increase in lattice recompression after unloaded shortening observed in both hypotonic conditions and the present experiments results chiefly from the altered geometrical relationship of the myofilaments, although a contribution arising from a reduction in ionic strength cannot be excluded, whereas the expansion of the lattice seen after prolonged stimulation results from osmolyte accumulation, and not from the action of an expansive cross-bridge radial force, which we show here remains compressive in these swollen fibers.

The authors thank Dr. H. Oetlicher for helpful discussions during the writing of the manuscript, the staff of the EMBL Outstation for expert assistance in performing this project, and the Wellcome Trust, CNR, Telethon, and the EU Large Installation Programme (CHGE-CT93-0040) for support.

REFERENCES

- Abbott, B. C., and R. J. Baskin. 1962. Volume changes in frog muscle during contraction. *J. Physiol. (Lond.)* 161:379–391.
- Allen, D. G., H. Westerblad, and J. Lännergren. 1995. The role of intracellular acidosis in muscle fatigue. *Adv. Exp. Med. Biol.* 384:57–68.
- April, E. W., P. W. Brandt, and G. F. Elliott. 1972. The myofilament lattice: studies on isolated fibres. The effects of osmotic strength, ionic concentration, and pH upon the unit-cell volume. *J. Cell Biol.* 53:53–65.

- Bagni, M. A., G. Cecchi, P. J. Griffiths, Y. Maéda, G. Rapp, and C. C. Ashley. 1994. Lattice spacing changes accompanying isometric tension development in intact single muscle fibres. *Biophys. J.* 67:1965–1975.
- Baskin, R. J., and P. J. Paolini. 1966. Muscle volume changes. *J. Gen. Physiol.* 49:387–404.
- Blinks, J. R. 1965. Influence of osmotic strength on cross-section and volume of isolated single muscle fibres. *J. Physiol. (Lond.)*. 177:42–57.
- Brenner, B., and L. C. Yu. 1991. Characterization of radial force and radial stiffness in Ca^{2+} activated skinned fibres of the rabbit psoas muscle. *J. Physiol. (Lond.)*. 441:703–718.
- Cecchi, G., M. A. Bagni, P. J. Griffiths, C. C. Ashley, and Y. Maéda. 1990. Radial component of cross-bridge force detected by lattice spacing changes in intact single fibres. *Science*. 250:1409–1411.
- Cecchi, G., P. J. Griffiths, M. A. Bagni, C. C. Ashley, and Y. Maéda. 1991. Time-resolved changes in equatorial x-ray diffraction and stiffness during rise of tetanic tension in intact length-clamped single muscle fibres. *Biophys. J.* 59:1273–1283.
- Curtin, N. A. 1986. Buffer power and intracellular pH of frog sartorius muscle. *Biophys. J.* 50:837–841.
- Curtin, N. A., C. Gilbert, D. M. Kretzschmar, and D. R. Wilkie. 1974. The effect of the performance of work on total energy output and metabolism during muscular contraction. *J. Physiol. (Lond.)*. 238:455–472.
- Dawson, R. M. C., D. C. Elliott, W. H. Elliott, and K. M. Jones. 1979. Data for Biochemical Research, 2nd Ed. Oxford University Press, Oxford.
- Dawson, M. J., D. G. Gadian, and D. R. Wilkie. 1977. Contraction and recovery of living muscles studied by ^{31}P nuclear magnetic resonance. *J. Physiol. (Lond.)*. 267:703–735.
- Godt, R. E., and D. W. Maughan. 1988. On the composition of the cytosol of relaxed skeletal muscle of the frog. *Am. J. Physiol.* 254:C591–C604.
- Godt, R. E., and T. M. Nosek. 1989. Changes in intracellular milieu with fatigue or hypoxia depress contraction of skinned rabbit skeletal and cardiac muscle. *J. Physiol. (Lond.)*. 412:155–180.
- Hendrix, J., H. Fuerst, B. Hartfiel, and D. Dainton. 1982. A wire per wire detector system for high counting rate x-ray experiments. *Nucl. Instr. Methods*. 201:139–144.
- Kushmerick, M. J. 1983. Energetics of muscle contraction. *Handbook Physiol.* 10:189–236. American Physiological Society, Baltimore.
- Lännergren, J. 1990. Volume changes of isolated *Xenopus* muscle fibres associated with repeated tetanic contractions. *J. Physiol. (Lond.)*. 420:116P.
- Lee, J. A., H. Westerblad, and D. G. Allen. 1991. Changes in tetanic and resting $[\text{Ca}^{2+}]$ during fatigue and recovery of single muscle fibres from *Xenopus laevis*. *J. Physiol. (Lond.)*. 433:307–326.
- Martell, A. E., and R. M. Smith. 1974. Critical Stability Constants, Vols. 1–6. Plenum, New York.
- Matsubara, I., and G. F. Elliott. 1972. X-ray diffraction studies on skinned single fibres of frog skeletal muscle. *J. Mol. Biol.* 72:657–669.
- Mobley, B. A., and B. R. Eisenberg. 1975. Sizes of components in frog skeletal muscle measured by methods of stereology. *J. Gen. Physiol.* 66:31–45.
- Nagesser, A. S., W. J. van der Laarse, and G. Elzinga. 1993. ATP formation and ATP hydrolysis during fatiguing intermittent stimulation of different types of single muscle fibres from *Xenopus laevis*. *J. Muscle Res. Cell Motil.* 14:608–618.
- Nagesser, A. S., W. J. van der Laarse, and G. Elzinga. 1994. Lactate efflux from fatigued fast-twitch muscle fibres of *Xenopus laevis* under various extracellular conditions. *J. Physiol. (Lond.)*. 481:139–147.
- Neering, I. R., L. A. Quesenberry, V. A. Morris, and S. R. Taylor. 1991. Nonuniform volume changes during muscle contraction. *Biophys. J.* 59:926–932.
- Perrin, D. D., and I. G. Sayce. 1967. Computer calculation of equilibrium concentrations in mixtures of metal ions and complexing species. *Talanta*. 14:833–842.
- Press, W. H., B. P. Flannery, S. A. Teukolsky, and W. T. Vetterling. 1989. Numerical Recipes: The Art of Scientific Computing. Cambridge University Press, Cambridge.
- Schoenberg, M. 1980. Geometrical factors influencing muscle force development: radial forces. *Biophys. J.* 30:69–78.
- Sillén, L. G., and A. E. Martell. 1971. Stability constants of metal ion complexes. Supplement no. 1, special publication no. 25. The Chemical Society, London.
- Tanokura, M., M. Imaizumi, and K. Yamada. 1986. A calorimetric study of Ca^{2+} binding by the parvalbumin of the toad (*Bufo*): distinguishable binding states in the molecule. *FEBS Lett.* 209:77–82.
- Veech, R. L., J. W. R. Lawson, N. W. Cornell, and H. A. Krebs. 1979. Cytosolic phosphorylation potential. *J. Biol. Chem.* 254:6538–6547.